

We are IntechOpen, the world's leading publisher of Open Access books Built by scientists, for scientists

6,900

Open access books available

186,000

International authors and editors

200M

Downloads

Our authors are among the

154

Countries delivered to

TOP 1%

most cited scientists

12.2%

Contributors from top 500 universities



WEB OF SCIENCE™

Selection of our books indexed in the Book Citation Index
in Web of Science™ Core Collection (BKCI)

Interested in publishing with us?
Contact book.department@intechopen.com

Numbers displayed above are based on latest data collected.
For more information visit www.intechopen.com



Quantification of Volumetric Changes of Brain in Neurodegenerative Diseases Using Magnetic Resonance Imaging and Stereology

Niyazi Acer¹, Ahmet Tuncay Turgut²,
Yelda Özsunar³ and Mehmet Turgut⁴

¹*Dept. of Anatomy, Erciyes University School of Medicine, Kayseri,*

²*Dept. of Radiology, Ankara Training and Research Hospital, Ankara,*

³*Dept. of Radiology, Adnan Menderes University School of Medicine, Aydın,*

⁴*Dept. of Neurosurgery, Adnan Menderes University School of Medicine, Aydın,
Turkey*

1. Introduction

In this chapter, we review the different magnetic resonance imaging (MRI)-based methods used to quantify whole and subcortical brain structures volume, and discuss the relevance of the brain atrophy in different neurodegenerative diseases. Although there are a lot of studies for multiple sclerosis (MS) and dementia of Alzheimer's type (AD) for the brain atrophy using different methods, the optimal method for quantifying atrophy has not been established to date.

In recent years, computed tomography (CT) scanning has been replaced with MRI scanning due to its enhanced soft-tissue resolution, especially for cerebrospinal fluid (CSF)-filled spaces, such as ventricular enlargement in patients with AD. Thus, a transition has occurred from CT to MRI in longitudinal studies investigating the human brain. As a result of development of new neuroimaging methods in clinical practice, volumetric methods started to be more sophisticated depending on various imaging methods (Lim et al., 2000). There are numerous reasons for the aforementioned transition; first of all, unlike CT, MRI has no inherent radiation effect, and secondly, CT underestimates cortical sulcal volume relative to MRI due to poorer resolution and spectral shift artifact on CT (Lim et al., 2000). Due to higher contrast resolution, MRI can better characterize the brain morphology including the size, tissue composition such as gray (or grey) matter and white matter, and shape of different cortical or subcortical neuroanatomic structures (Lim et al., 2000). Nowadays, it is possible to use MRI to visualize and quantify the directional coherence of white matter fibers, called diffusion tensor imaging (DTI), for investigation of connectivity and disconnectivity between different brain regions (Basser et al., 1994). Additionally, MRI equipments are also used to provide functional brain responses with functional MRI (fMRI) and perfusion MRI as in some nuclear medicine neuroimaging methods such as positron emission tomography (PET) and single photon emission computed tomography (SPECT). These methods can provide pathognomonic data of certain structural lesions in AD, as they can demonstrate neuronal activity or receptor characteristics (Small, 2002). High field MRI

has started to further depict the regional atrophy patterns AD and other neurodegenerative disorders.

In this chapter, we aim to overview the challenging and exciting radiological methods used for the diagnosis of various neurodegenerative diseases. Specifically, we focus on the neuroimaging techniques in the first part of the chapter, their clinical applications in the second part, and methods for volume estimation including stereological techniques on the last part of the text.

2. Neuroimaging techniques

Primary neuroimaging techniques that are widely used clinically are CT, PET, SPECT, conventional MRI, fMRI, magnetic resonance spectroscopy (MRS), and tractography or DTI. These techniques enlighten different aspects of brain structures or functions (Frey et al., 1999; Small, 2002). An overview of the neuroimaging techniques is following:

2.1 Computed tomography (CT)

CT is the first imaging modality to provide *in vivo* evidence of the brain atrophy in different neurodegenerative diseases. CT images are generated by passing an x-ray beam through the skull or other object (e.g. spine and vertebral column) and it measures the attenuation of an x-ray beam through different body tissues e.g. brain, bone and CSF. Therefore, tissue's appearance will vary according to degree of its attenuation (Frey et al., 1999). The degree of attenuation can be measured numerically as a tissue density number for each voxel (volume element) and then these numbers can be converted to gray scale values and presented visually as pixels (Frey et al., 1999). Among different body tissues, the bone has the highest attenuation and appears white on CT images (Small, 2002). On the other hand, CT study has some limitations such as radiation hazards, inability to differentiate gray and white matter due to low contrast resolution and visualization of the posterior fossa structures, particularly brain stem and cerebellum. Despite to these limitations, quantitative CT still can demonstrate the presence of greater brain atrophy and ventricular dilatation in patients with AD compared with controls (Creasey et al., 1986).

2.2 Single photon emission computed tomography (SPECT)

In SPECT, the scanner determines the site of the photon source following administration of an unstable isotope or inhaled/injected tracer and thus an image reflecting cerebral blood flow or receptor distribution is produced (Schuckit et al., 1992). Unfortunately, its spatial resolution is not high enough for imaging deep structures and determination of the source of single photon emitters is difficult (Small, 2002).

2.3 Positron emission tomography (PET)

A PET scanner determines the line along which the photons travel, by recording the simultaneous arrival of two different photons at different detectors, and an image is then constructed from information received by the scanner. Importantly, PET study demonstrates receptor characteristics like density and affinity following injection of receptor ligands labeled with nuclides, in addition to cerebral blood flow. In patients with AD, PET studies using fluorodeoxyglucose have revealed characteristic alterations in cerebral blood flow and metabolism in the parietal, temporal and prefrontal cortices (Mazziotta et al., 1992).

2.4 Conventional magnetic resonance imaging (MRI)

The MRI scanner detects the radiofrequency energy emitted and energy level changes represent different brain structures. Typically, T1-weighted images differentiate gray and white matter, while T2-weighted images delineate white matter hyperintensities. It is reported that spatial resolution for MRI is 1 to 2 mm, less than that of CT (Small, 2002). Fortunately, patients can have multiple MRI scans because it does not involve ionizing radiation. In MRI study, the object is placed in a high field strength magnetic field varying from 0.5 to 3 Tesla (T). Technically, different relaxation times, in addition to proton density, are measured and further manipulations by using various pulse sequences are possible. Today, various MRI techniques such as fast spin echo, high performance gradients, echo planar and diffusion weighted imaging are available for clinical use, in addition to MRI contrast agents, CSF velocity analysis, and interventional MRI (Bradley & Bydder, 1997). Recently, some technical improvements regarding the acquisition and processing of structural data have provided vivid visual representations of the external surface and internal structures of the human brain (Lim et al., 2000). Clinically, the progressive neuronal loss leading to atrophy in neurodegenerative disease increases the value of MRI (Loewe et al., 2002).

2.5 Functional magnetic resonance imaging (fMRI)

With recent developments in MRI techniques, it is also possible to measure brain activity and tissue signal changes, reflecting local changes in oxygenation of haemoglobin, which depend on regional blood perfusion. Technical point of view, the signal intensity of deoxygenated hemoglobin differs from that of oxygenated hemoglobin (Belliveau et al., 1992). This MRI method also called BOLD technique. As a rule, the brain tissue during brain activity does not use this excess oxygen, causing high concentration of oxygenated blood, greater levels of magnetic field homogeneity and higher MRI signal intensity (Wagner et al., 1998). Thus, brain regions receiving greater blood flow during brain activity produce a stronger MRI signal than do other regions and areas of relative brain activity can be easily detected (Small, 2002).

2.6 Diffusion tensor imaging (DTI)

DTI provides detailed information concerning the anatomy of white matter structure in the central nervous system. With use of DTI, visualizations of projections of axonal fibers, i.e. neuronal connectivity, is possible by quantitative evaluation on the anisotropy of water diffusion, local fiber orientation and integrity of white matter tracks (Jones et al., 1999). Technically, DTI visualizes diffusional anisotropy within each voxel as three-dimensional projections of axonal fibers. In patients with AD and other neuropsychiatric disorders, the degree of neuronal connectivity loss is a useful marker in the progression of the disease (Buchsbaum et al., 1998; Ewers et al., 2011). Moreover, recent studies revealed the presence of loss of myelin and axons in patients with AD, particularly periventricular areas (Hanyu et al., 1997; Ewers et al., 2011).

2.7 Magnetic resonance spectroscopy (MRS)

From the technical view, the magnetic resonance spectrum display according to frequency shows different chemical forms of the element such as characteristic peaks, thus reflecting tissue metabolite concentrations (Weiner, 1987; Bothwell & Griffin 2011). As a noninvasive study, MRS provides quantitative regional biochemical and physiologic features of the

tissue. To determine *N*-acetylaspartate (NAA) content of hippocampus in patients with AD, some authors used proton MRS (¹H MRS) and volumetric MRI (Weiner, 1987; Schuff et al. 1997).

2.8 Improvements in magnetic resonance imaging

2.8.1 Mechanisms of tissue contrast: Pulse sequences

By varying elements of the image acquisition sequence of MRI, it is possible to manipulate the amount of contrast between various tissues. It is well-known that hydrogen atoms are the most important element of the tissue and MRI device demonstrate signals related with free water. Based on proton density and relaxation time of any tissue, different structures will appear in an acquired image. T1 means the time taken for excited nuclei to return to equilibrium, while T2 is an exponential time constant related with the time for the excited nuclei to lose signal (Lim et al., 2000). Technical view of point, the time between radiofrequency pulses (TR) and the amount of time after the pulse called echo time (TE) are important parameters; a long TR and a long TE give T2-weighted image, while a short TR and a short TE gives T1-weighted image. Although T1-weighted spin-echo and inversion recovery sequences have poor definition of CSF/skull margins for reliably measuring intracranial volume, they are used for morphometric studies because they provide good white-gray contrast (Lim et al., 2000).

Sources of contrast other than that based on manipulation of T1, T2, fluid-attenuated inversion recovery (FLAIR) and proton density are used to obtain further information. T1-weighted images are superior to T2-weighted images for the evaluation of atrophy, because T2-weighted ones overestimate the dimensions of ventricles and sulci (Kucharczyk & Henkelman, 1994). On the other hand, T1-weighted imaging gives a clear distinction between grey matter, white matter and CSF; therefore, they are used for quantitative MRI studies of brain morphology, particularly of individual brain structures (Keller & Roberts, 2009) (Fig. 1).

Fast spin echo T2 sequences has been usually used in brain imaging due to their short acquisition time and increased robustness to motion artifacts. In imaging of neurodegenerative disorders like Parkinson-like syndromes, however, gradient echo T2-weighted spin-echo sequences are preferred because they increase the sensitivity for paramagnetic materials (ferritin, melanin etc.). Also, proton-density or FLAIR sequences identify gliosis owing to result of progressive neuronal loss (Loewe et al., 2002). Therefore, T2-weighted imaging may be used for determination of intracranial volume as the increased signal intensity of CSF provides better determination of CSF and the parenchyma of the brain (Keller & Roberts, 2009). Therefore, the type of MRI sequence used is important for volume estimation.

2.8.2 Two-dimensional multi-slice and three-dimensional imaging

Two-dimensional (2D) images are obtained in axial, sagittal and coronal planes (Fig. 1). Image orientation, giving a different view of the brain with optimal visualization of different structures, is described according to radiofrequency pulse excitations and the magnetic gradients in three orthogonal axes. Basically, a mid-sagittal section provides an image of the corpus callosum and the prefrontal cortex, coronal section gives an image of the limbic structures including hippocampus, and axial section gives an image of basal ganglia structures and the lateral ventricular system.

It is important to know that 2D image has a limitation so that only selected slices imaged and therefore a comparison across subjects is difficult, although it may be possible by orienting each slice acquisition relative to a specific anatomic plane. On the other hand, three-dimensional (3D) volume acquisition protocols include the entire brain and they are widely used in psychiatric neuroimaging. Using T1-weighted MRI sections with a good gray/white matter differentiation, the entire brain with 1.5 mm or thinner slices are obtained in 10 minutes or less. As a rule, an in-plane resolution of 1 mm means that each pixel in the image matrix represents 1 mm² (Lim et al., 2000).

Quantitative investigations of the brain using MRI may reveal important information about the function and organisation of the brain being studied, recently. MRI has become the method of choice for the examination of macroscopic neuroanatomy in vivo due to excellent levels of image resolution and between tissue contrasts. Estimation of brain compartment volume needs high resolution MRIs for the delineation of anatomical boundaries. With the use of higher magnetic field strength, a better image quality with can be obtained using thinner slices and shorter imaging time. For this reason, many researchers frequently use MRI scanners which are either with 1.5 T or 3 T systems (Fig. 2). Although 3 T systems offer increased resolution of between-tissue contrast (i.e. increased visualisation of the borders between gray matter, white matter and CSF), MRI scans on 1.5 T systems are sufficient for the quantification of relatively small brain structures, such as the hippocampus, amygdala, and deep gray matter nuclei (Keller & Roberts, 2009).

3. Clinical applications

3.1 Dementia syndromes

A number of studies reported that patients with MS have smaller volumes of the parenchyma than in age-matched control subjects (Bermel et al., 2003; Sanfilipo et al., 2005, 2006). The first method used for the estimation of brain atrophy is linear measurement of ventricles or other brain structural dimensions (Smith et al., 2002). In general, MRI studies reveal some differences in the volume of the brain structures in certain neurodegenerative diseases, an inhomogeneous group of neurological diseases with unknown etiology, such as demantia. In such diseases, multiple systems or one system or one group of nuclei may partly or totally be involved (Loewe et al., 2002). Basically, there are two principal pathological processes which determine imaging findings: neuronal or white matter loss and deposition of different compounds. The loss of neurons leads to progressive atrophy associated with white matter loss and gliosis (Kern & Behl, 2009).

Nowadays, dementia is a well-known illness with a high incidence in the aged population. Clinically, there are a number of neurodegenerative diseases causing dementia, including AD, dementia with Lewy bodies, and frontotemporal dementia. Furthermore, dementia picture is also present in some neurodegenerative illnesses including Creutzfeldt-Jakob disease, Huntington's disease, progressive supranuclear palsy, multiple system atrophy, amyotrophic lateral sclerosis, and Parkinson's disease (Loewe et al., 2002; Vitali et al., 2008).

3.1.1 Alzheimer disease (AD)

AD is well-known progressive neurodegenerative pathology, accounting for around 60% of all cases dementia. Clinically, patients with AD have serious cognitive findings related with memory, language, such as confusion, poor judgment, language disturbance, agitation, withdrawal, and hallucinations (Mohs & Haroutunian, 2002).

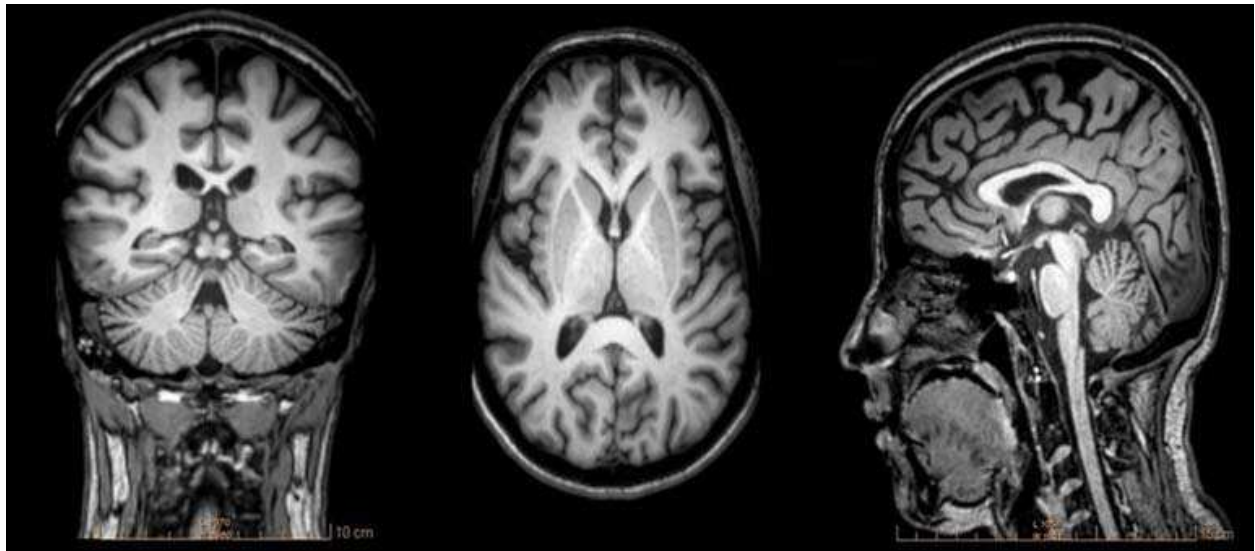


Fig. 1. T1-weighted MRI scans acquired in coronal (left), axial (center) and sagittal (right) planes with 3 T. All images were acquired with a field of view of 25 cm and 256 x 256 matrix, 1-mm slice thickness. Image was acquired using a turbo field echo sequence, gated to achieve an effective TR of >8 ms and TE of 4 ms. Left: Coronal image passing through lateral ventricles and temporal lobes. Center: Axial image passing through the lateral ventricles and basal ganglia. Right: Mid-sagittal image highlighting the corpus callosum, brain stem and cerebellum

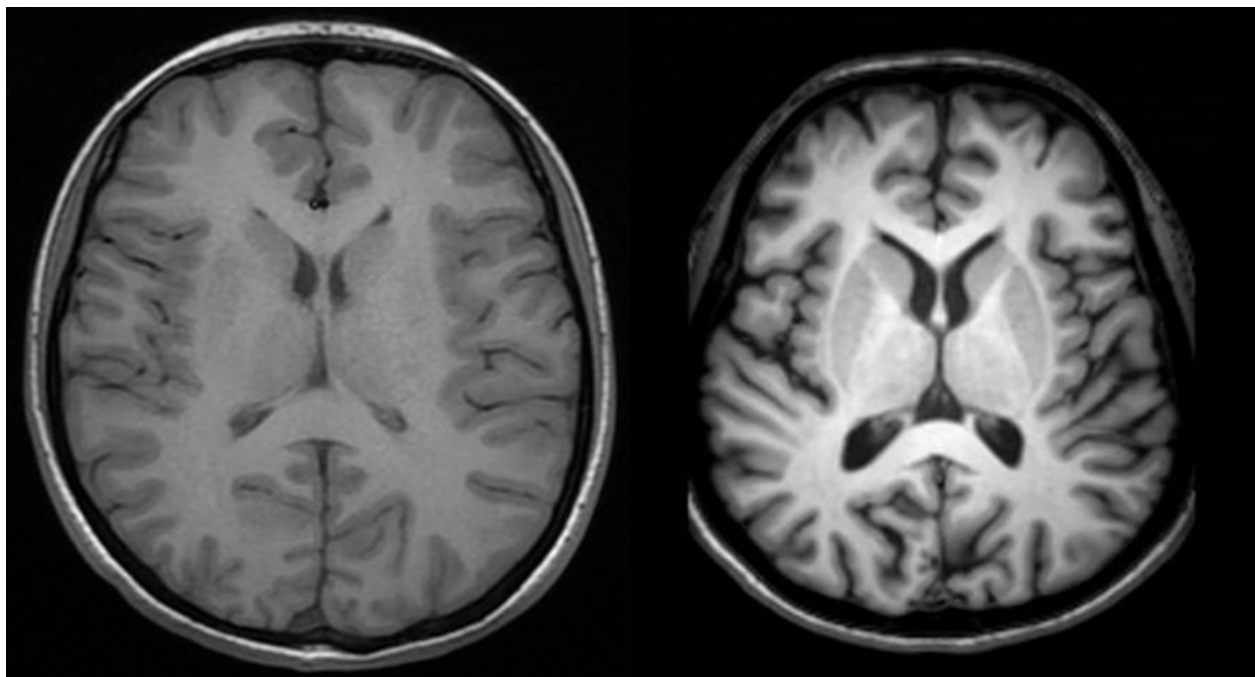


Fig. 2. T1-weighted axial MRIs acquired with 1.5 T (left) and 3T (right) MRI scanners. 3T MRI was acquired with a field of view of 25 cm and 256 x 256 matrix, 1-mm slice thickness. Image was acquired using a turbo field echo sequence, gated to achieve an effective TR of >8 ms and TE of 4 ms. 1.5T MRI was acquired with field of view of 24 cm, 1.5 mm slice thickness. Image was acquired using a spoiled gradient recalled acquisition sequence, gated to achieve an effective TR of >35 ms and TE of 15 ms

Gross examination of the brain in patients with AD demonstrated an obvious atrophy, widening of the sulci, and erosion of the gyri. Histologically, the atrophy of the cortex is associated with significant reductions in the numbers of neurons. Macroscopically, the weight of the brain is decreased compared to normal controls (Masliah et al., 1991). In a previous study using unbiased stereologic sampling techniques, about 50% loss in neurons of the superior temporal gyrus has been reported (Gomez-Isla et al., 1996, 1997). In another study, 40-46% loss of large neurons in the frontal and temporal cortices of specimens has been reported in patients with AD (Terry et al., 1981). In fact, neuronal loss and degeneration are not restricted to the cortex; it may be observed in subcortical nuclei such as the locus ceruleus, raphe aminergic nuclei (Zweig et al., 1988; Chan-Palay & Asan, 1989), and the nucleus basalis of Meynert (Whitehouse et al., 1982). In such cases, synaptic markers such as synaptophysin are significantly reduced in the cerebral cortex, especially the frontal and parietal cortices and in the hippocampus, with increasing age (Nagy et al., 1995).

Radiologically, MRI provides understanding of disease progression in AD and other dementias. Recently, it has been reported that patients with AD have atrophy in parietal lobes, medial temporal lobe and hippocampus on MRI (Loewe et al., 2002, Vitali et al., 2008). The parietal lobe atrophy is observed on axial or coronal T1-weighted or FLAIR sequences with thinning of the posterior part of the body of the corpus callosum on T1-weighted sagittal sequences (Yamauchi et al., 2000). In some studies, decreased hippocampal and entorhinal cortex (ERC) volumes in patients with AD were noted (Appel et al., 2009). Hippocampal atrophy is observed with thin coronal T1-weighted or FLAIR tomographic slices through the medial temporal lobes (Teipel et al., 2003). A lot of quantitative MRI studies indicate that white matter hyperintensities correlate with neuropsychological functioning in both healthy elderly persons and demented patients (Boone et al., 1992; Lopez et al., 1992). Other studies indicate loss of cerebral gray matter (Rusinek et al., 1991), hippocampal and parahippocampal atrophy (Kesslak et al., 1991), and lower left amygdala and ERC volumes in patients with AD (Pearlson et al., 1992; O'Brien, 2007).

Recently, a longitudinal study demonstrated that most common neuropathologic findings in elderly patients are neuritic plaques and neurofibrillary tangles (Mohs & Haroutunian, 2002). The presence of these findings before clinical AD diagnosis suggests that *in vivo* methods that directly image these pathognomonic lesions would be useful presymptomatic detection technologies (Mohs & Haroutunian, 2002).

3.1.2 Frontotemporal demantia (FTD)

Frontotemporal demantia (FTD) is as common a cause of dementia. In particular, volumes of some regions of the frontal lobe (the ventromedial and posterior orbital regions of the frontal lobe), the cingulate cortex, and the insula are reduced in patients with the FTD, compared with those of both AD patients and age-matched controls. This feature differentiates this illness from AD as these areas are relatively spared in the latter disease (Rosen et al., 2002). In patients with the semantic variant of FTD, there is a relative preservation of frontal lobe volumes but marked loss of volumes in the temporal lobes (Rosen et al., 2005, 2006). In clinical practice, FTD includes a group of neurodegenerative diseases characterized by focal atrophy of frontal and anterior temporal lobes and non-AD pathology (Neary et al., 1998; McKhann, 2001; Ratnavalli, 2002).

3.1.3 Dementia with Lewy bodies (DLB)

Dementia with Lewy bodies results a diffuse, irreversible and destructive atrophy (Seppi & Schocke, 2005). Measurement of brain volume to predict atrophy using MRI may be used as

a predictor for outcome in different neurodegenerative diseases such as AD. There are a lot of biologic factors influencing cerebral volume measurement such as inflammation and edema, cerebrovascular disease, chronic alcoholism and normal aging (Ron et al., 1982; Molyneux et al., 2000).

3.2 Multiple Sclerosis (MS)

In cases with MS, various measurement techniques revealed atrophy of brain and spinal cord, axonal loss, and Wallerian degeneration (Sharma et al., 2004). Recent studies show that the MS is a destructive disease process and whole-brain atrophy is a valuable marker for the progression of the disease (Sharma et al., 2004).

3.3 Medial temporal lobe epilepsy (MTLE)

In patients with medial temporal lobe epilepsy (MTLE), the atrophy of the hippocampus is often observed on routine MRI. Recently, it has been reported that automatic morphometry can be used as a clinical tool to provide a quantifiable estimation of hippocampal atrophy in patients with MTLE (Bonilha et al., 2009). Most recently, Henry et al. (2011) suggested that ultrahigh-field-strength MRI revealed prominent atrophy of Ammon horn in patients with MTLE and hippocampal sclerosis.

3.4 Ageing

With increasing age, there are some volumetric changes in the gray matter structures of the temporal lobe, amygdale, and hippocampus, a critical structure for memory in AD, but they are heterogenous, with some regions showing more atrophic changes than others (O'Sullivan, 2009). Recently, it has been reported that it is possible to differentiate ageing from AD with 87% accuracy (Likeman et al., 2005; O'Sullivan, 2009). Some volumetric studies demonstrated that changes in white matter regions provide an early and accurate diagnosis (Davatzikos et al., 2008).

4. Methods for volume estimation

4.1 Manual, automated and semiautomated methods for volume estimation

Use of imaging methods for quantitative volume estimation such as manual, semi-automated and automated methods can provide the capability to reliably detect and identify general and specific structural abnormalities of the brain. Use of these methods can aid to diagnose some specific neurological diseases and facilitate monitoring of the progression of the disease. Quantitative measures of the brain atrophy can be clinically relevant and much work has been carried out to establish diagnosis of AD (Furlong, 2008).

At present, a number of manual, semi-automated and automated methods based on conventional MRI are available for measuring whole or regional brain volume. Ideally, the technique for measuring tissue volume should be reproducible, sensitive to subtle modifications, practical, fast and correct. Theoretically, many factors may affect the quantification of brain atrophy using segmentation methods, such as the pulse sequence and the resolution parameters chosen for the acquisition (Horsfield et al., 2003; Sharma et al., 2004).

One of these most important factors is slice thickness. The use of thin slice helps to reduce the partial volume effect and consequently permits a better estimation of tissue volumes. Moreover, high contrast makes segmentation between the different cerebral compartments

easier. Depending on the compartment of interest, tissue contrast can be chosen such as CSF/parenchyma or gray/white matter (Grassiot et al., 2009). There are many different segmentation methods for estimating brain volume using manual or automated techniques. Flippi et al. (1998) used manual technique for whole brain volume with MS. Although the manual tracing of brain structure allows brain volume to be estimated, this technique is a time consuming method (Flippi et al., 1998).

Semi-automated techniques, quicker and more reproducible, use various algorithms of brain segmentation from 3D volume (Horsfield et al., 2003). For both semi-automated and automated methods, however, manual defining of brain structures is necessary. In semi-automated methods, manual marking of some anatomical landmarks and an automatic segmentation of the region of interest (ROI) are required, while automated methods are completely user-independent in the determination of various parameters such as brain size and shape. Importantly, experienced raters with detailed knowledge of neuroanatomy are necessary for manual techniques and correct estimations related to the neuroanatomical ROI are possible (Keller & Roberts, 2009).

Automated and semi-automated methods for segmentation and quantification of the brain are used in most studies. More recently, various image analysis tools have been developed, including both automated and semi-automated algorithms, relying on either raw or normalized brain volume assessments (Pelletier et al., 2004). Several previous studies have described automatic segmentation methods using MRIs. Calmon & Roberts (2000) reported a segmentation method for the lateral ventricles on coronal MR images. Stokking et al. (2000) described the development of a morphology-based brain segmentation method for fully automatic segmentation of the brain using T1-weighted MRI data. Webb et al. (1999) reported a method of automatic detection of the hippocampus with atrophy. These methods each segmented one target object on each MRI obtained by different sequences. Therefore, these methods could not segment two or more objects simultaneously on MRIs obtained by a single sequence.

There are two primary methods for manual quantification of brain compartment volume from MRIs, namely stereology in conjunction with point counting and planimetric methods or manual tracing (Acer et al., 2007; Keller & Roberts, 2009). Authors used manual tracing of brain boundaries from MRI scans using various softwares such as Analyze (Biomedical Imaging Resource, Mayo Foundation), BRAINS (Iowa Mental Health Clinical Research Center 2008), and FreeSurfer (Dale et al., 1999; Fischl et al., 1999; Fischl et al., 2002). Manual techniques such as planimetry or tracing methods require the investigator to delineate a brain region based on reliable anatomical landmarks, whilst the software package provides information on volume. Tracing methods require the investigator to trace the brain ROI using a mouse driven cursor throughout a defined number of MRI sections (Keller & Roberts, 2009). The cut surface areas, determined by pixel counting within the traced region, are summed and multiplied by the distance between the consecutive sections traced to estimate the total volume. Although tracing methods represent the most commonly used tool to estimate brain structure volume on MRIs, there are some drawbacks associated this technique (Geuze et al., 2005). Firstly, the time taken to perform manual tracing or manual segmentation methods is significantly longer than stereological point counting methods (Acer et al., 2007, 2008; Keller & Roberts, 2009). Secondly, tracing and manual segmentation methods suffer from the risk of "hand wobble" during the delineation of ROI boundaries on MRI sections (Keller & Roberts, 2009).

The measurement of rates of change requires volume quantification. In general, manual or semi-automated methods have been employed for volume quantification on structural brain

MRIs, but they are generally severely limited in practicality and reliability. For example, a high-resolution 3D brain MRI data set can contain more than 100 slices to cover an entire brain (Keller & Roberts, 2009). Manually delineating tissue boundaries for volumetric measurement can be a tedious and demanding process because of the presence of the extremely complex convoluted structures of the brain. Manual tracing is also well-known to be associated with large subjective variability and low reproducibility. As a result, methods with better reproducibility and higher precision are required for measuring subtle neuro-anatomic changes and these methods are likely to be based on computerized approaches. FreeSurfer is freely available on the World Wide Web (www or commonly known as the Web), it has been widely used in the neuroimaging field. At present, fully automated methods are most often used. Fully automated or semi-automated methods can be applied to a specific ROI (such as the thalamus or the hippocampus) to obtain a regional brain volume (Houtchens et al., 2007).

4.2 Brain segmentation

Brain tissue segmentation of MRIs means to specify the tissue type for each pixel or voxel in a 2D or 3D data set, respectively, on the basis of information available from both MRIs and the prior knowledge of the brain. It is an important preprocessing step in many medical research and clinical applications, such as quantification of tissue volume, visualization and analysis of anatomical structures, multimodality fusion and registration, functional brain mapping, detection of pathology, surgical planning, surgical navigation, and brain substructure segmentation (Suri et al., 2002). So far, various segmentation techniques such as Gaussian mixture models (Ashburner & Friston, 2005), discriminant analysis (Amato et al., 2003), k-nearest neighbor classification (Mohamed et al., 1999), and fuzzy c-means clustering (Pham & Prince, 1999; Suckling et al., 1999; Ahmed et al., 2002; Zhou & Bai, 2007) were used to determine gray and white matter volume. Most recently, it has been reported that "fuzzy" cluster or classifier approaches were found to have a high reliability, accuracy, and validity (Herndon, 1998).

4.3 Image processing and segmentation

Today, medical image processing and segmentation are used to improve the quality of diagnosis. We can calculate the cortical volume and surface area using the Fuzzy C-Means algorithm as a semi-automated segmentation method as described in Figure 3.

Firstly, T1-weighted MRIs are normalized using registration algorithms. Following normalization process, we obtain brain contour to calculate volume and surface area of the brain using image working algorithms. Images of brain are cleared brain contour using morphological image processing. This method involves two major steps and final segmented images result from separation of parenchyma for brain volume and surrounding line for cortical surface area of the brain (Tosun et al., 2004; Ueda et al., 2009; Brouwer et al., 2010; Lui et al., 2010) (Fig. 4).

4.4 Stereological approaches

In general, stereological methods provide quantitative data on 3D structures using 2D images. Stereological methods have been widely applied on MRIs to estimate geometric variables, such as volume and surface area, and various internal brain compartments. The volume of internal brain structure can be obtained using the Cavalieri principle of stereologic approaches.

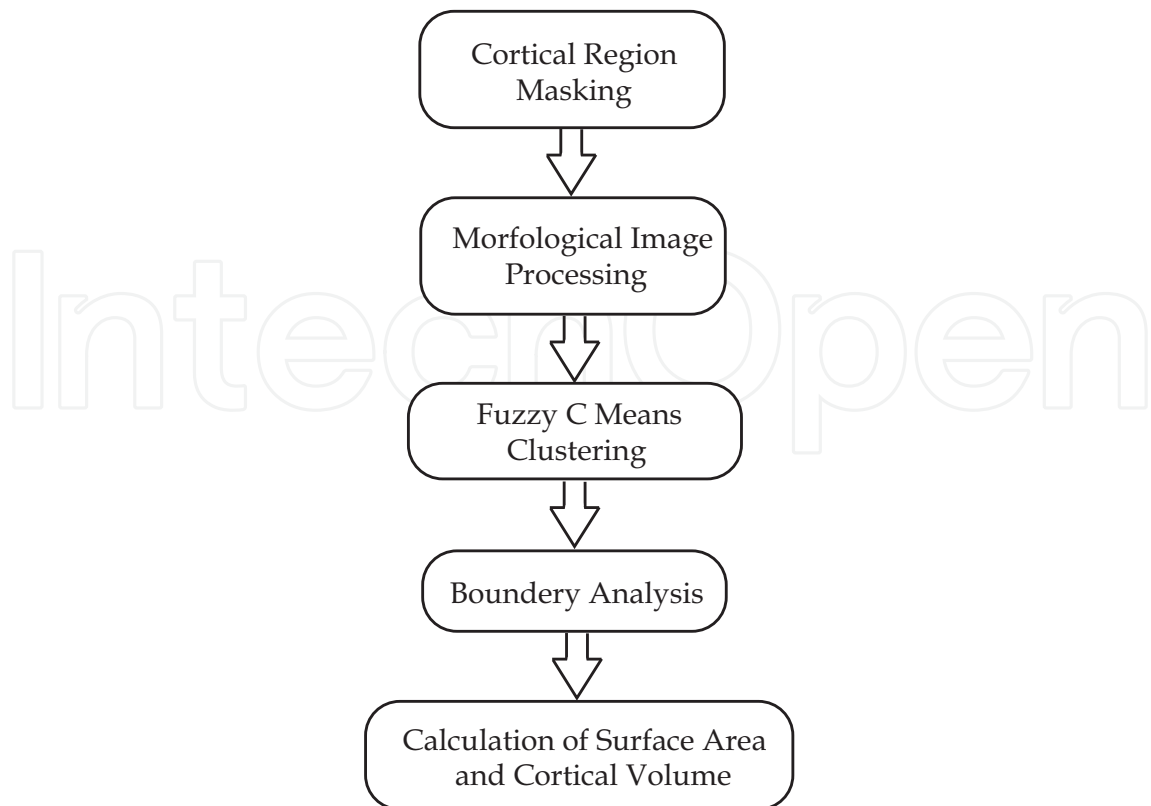


Fig. 3. Brain image segmentation blocks (Nakamura & Fisher, 2009)

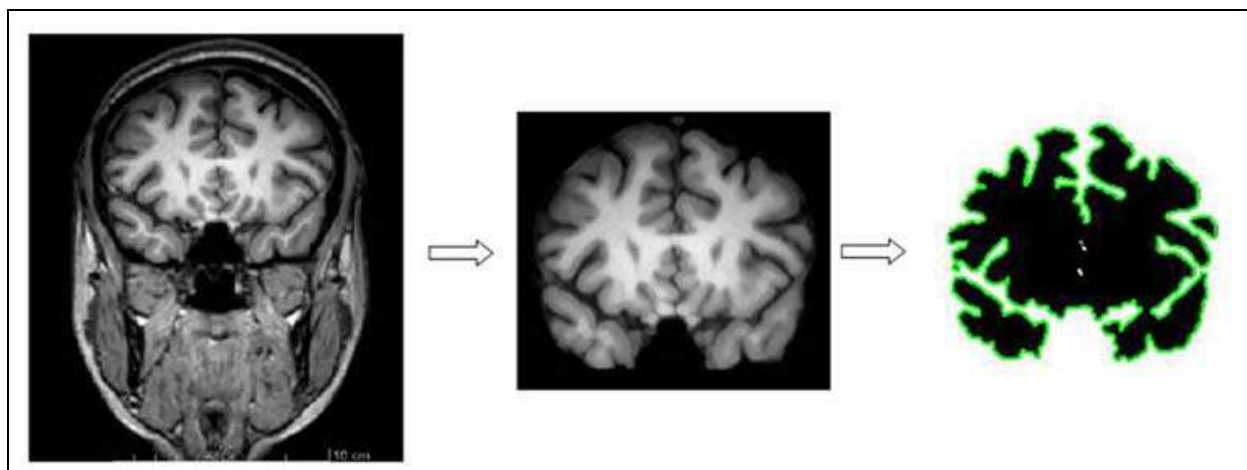


Fig. 4. Segmentation called the Fuzzy C. Left: Original T1-weighted image. Center: Masking and removal of artifacts the outer contour of the brain. Right: Contour of segmented image is outlined

4.4.1 Point-counting method

The Cavalieri method in combination with point counting requires beginning from a uniform random starting within the sectioning interval, a structure of interest is exhaustively sectioned with a series of parallel plane probes a constant distant apart. An unbiased estimate of volume is obtained by multiplying the total area of all sections through the structure by sectioning interval t as following:

$$estV = t \times (a_1 + a_2 + \dots + a_n) \quad (1)$$

where a_1, a_2, \dots, a_n show the section areas and t is the sectioning interval (Roberts et al., 2000; García-Fiñana et al., 2003).

The point counting method involves overlying each MRI with a regular grid of test points. After each superimposition, the number of test points hitting the structure of interest is counted on each section and we can estimate volume following formula:

$$estV = t \times \left(\frac{a}{p} \right) \times (p_1 + p_2 + \dots + p_n) \quad (2)$$

where p_1, p_2, \dots, p_n show point counts and a/p represent the area associated with each test point. To avoid bias, the position of the test system should be uniform randomly (Roberts et al., 2000; García-Fiñana et al., 2003).

In any case, the following formula (Eq.3) can be used for volume estimation from MRIs of the brain (Şahin & Ergür, 2006; Acer et al., 2008):

$$V(pc) = t \times \left[\frac{su \times d}{sl} \right]^2 \times \sum p \quad (3)$$

where ' t ' is the section thickness, ' su ' the scale unit of the printed film, ' d ' the distance between the test points of the grid, ' sl ' the measured length of the scale printed on the film and ' $\sum p$ ' is the total number of points hitting the sectioned cut surface areas of the related structures such as the cerebrum.

From stereological point of view, planimetry and point-counting are two different methods for estimating volume based on the Cavalieri principle. The Cavalieri principle may be used for estimating the volume of brain and substructures such as hippocampus, amygdale and thalamus. Therefore, a random beginning is necessary and the object is cut into slices of a known and fixed thickness. The volume is estimated by multiplying the distance between the slices by the total cut area of the structures are under investigation. The cut area of the structures may be estimated by point-counting or planimetry. Nevertheless, the Cavalieri principle in combination with point-counting is ideal for estimating total volumes of various brain and any compartments. Keller et al. (2002, 2007, 2008) and Acer et al. (2008, 2010) have previously applied this technique to obtain volume estimations of various brain structures such as Broca's area, hippocampus, ventricles, cerebral hemisphere, and cerebellum. In these studies, a set of parallel and equidistant MRIs of the brain is randomly selected, and the ROI is directly estimated on each image by randomly superimposing a grid of points, and subsequently, counting the number of points that fall within the ROI (Keller et al., 2002, 2007, 2008; Acer et al., 2008, 2010).

Stereology in combination with point counting has an advantage related with the time taken to estimate volume of brain structures on MRIs. Compared with manual tracing or segmentation methods, this technique is much more time efficient. Another advantage of stereology in combination with point counting is the prediction of the coefficient of error (CE) so that it may be used to identify the optimal parameters of sampling needed to achieve a given precision such as we need the number of MRI sections and the density of the point grid.

Importantly, the stereological approach provides an opportunity for the investigator making appropriate changes on their sampling or estimating procedures. Therefore, the Cavalieri

method gives a CE of estimation for each volume assessment. Thus, an investigator may easily observe the potential variability in any given volume measurement. It may cause some problems in accuracy and hence interpretation in the presence of high CE for these measurements. If too few slices or too few points are taken for volume estimation, it is possible to encounter with such problems. The investigator is eligible to change the spacing of points in the grid or the number of slices available in any CT or MR study to provide a reasonable CE value. More importantly, an appropriate grid size and the number of slices required for volume estimation of an object is crucial at the beginning, obviating the need to calculate the CE value for repeated sessions (Sahin et al., 2003; Acer et al., 2008).

In the stereological method, continuous investigator computer interaction is necessary because all points intersecting the cerebral hemispheres should be removed or marked on consecutive MRI sections. For the reliable measurement of each brain structure using stereology in conjunction with point counting, the stereological parameters like grid size and slice gap should be optimized by counting at least 200 points per structure. In a previous study investigating the cerebral hemispheres, a grid size of 15 and slice gap of every 15 sections results in approximately 200 points being counted per hemisphere on frequently acquired 3D T1-weighted images (Mackay et al., 1998; Cowell et al., 2007), and it achieves a CE lower than the optimal 5% (Roberts et al., 2000). It has been reported that stereological volume estimation of a cerebral hemisphere using the Windows based software packages (EASYMEASURE and MEASURE) takes approximately 10 minutes (Keller & Roberts, 2009).

Stereological point counting method involves the random placement of a grid with sufficient resolution in 2D or 3D over the structure of interest and counting the points overlying the ROI. For this method, the requirements are a grid encompassing the region or structure completely, the structure placed with a grid randomly, and an adequate number of points counted on an adequate number of slices. Thus, the stereological point counting approach is very efficient and statistically sound, in addition to providing a CE of the measurement of the volume of the structure of interest.

4.4.2 Worked example for point-counting technique

According to point-counting technique, a square grid of test points is positioned on each MRI section, and all points hitting the cerebrum are counted (Fig. 5).

T = 1.6cm, d = 0.8cm, SU=8 cm, SL=7.8 cm, ΣP = 796

$$V(pc) = t \times \left[\frac{su \times d}{sl} \right]^2 \times \sum p \tag{3}$$

$$V = 1.6 \times \left[\frac{8 \times 0.8}{7.8} \right]^2 \times 796 = 856.90cm^3$$

In the Cavalieri method in combination with point-counting technique using MRI sections, relationship between numbers of section and counts is given in Table 1.

Section number	1	2	3	4	5	6	7	8	Total Point Counts
Point number	42	72	122	132	129	116	115	68	796

Table 1. Relationship between numbers of section and counts of point in point-counting technique

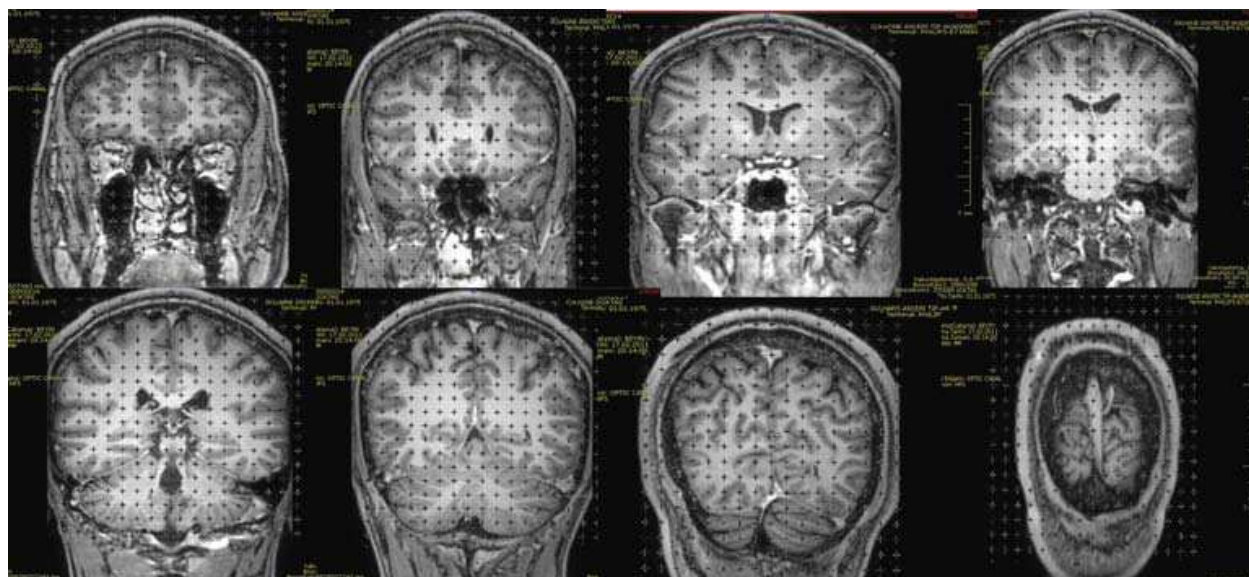


Fig. 5. Acoronal MRI series with a point-counting on it for the estimation of the cerebral volume from first to last section ($T=1.6$ cm)

4.4.3 Error prediction for point counting technique

The error predictors given below originate from the recent literature (García-Fiñana & Cruz-Orive, 2000; Garcia Finana, 2006; Garcia Finana et al., 2009). In particular, the estimation of volume and variance of the volume estimate for the cerebral volume are calculated as follows.

An unbiased estimator of Q can be constructed from a sample of equidistant observations of f , with a distance T apart, as follows:

$$\hat{Q}_T = T \sum_{k \in Z} f(x_0 + kT) = T(f_1 + f_2 + \dots + f_n) \quad (4)$$

where x_0 is a uniform random variable in the interval $[0, T)$ and $\{f_1, f_2, \dots, f_n\}$ is the set of equidistant observations of f at the sampling points which lie in $[a, b]$. In many applications, Q represents the volume of a structure and $f(x)$ is the area of the intersection between the structure and a plane that is perpendicular to a given sampling axis at the point of abscissa x (García-Fiñana & Cruz-Orive, 2000; Garcia Finana, 2006; Garcia Finana et al., 2009).

This data sample represents the area of cerebrum in cm^2 on a total of 8 MRI sections a distance $T = 1.6$ cm apart (Table 1).

To estimate $\text{Var}(\hat{Q}_T)$ via Eq. (5) we have to calculate first $\alpha(q)$, C_0 , C_1 , C_2 and C_4 (Table 2).

$$\text{var}(\hat{Q}_T) = \alpha(q)(3C_0 - 4C_1 + C_2)T^2 \quad q \in [0, 1] \quad (5)$$

From Eq. (6), we have:

$$C_k \sum_{i=1}^{n-k} f_i f_{i+k}, \quad k = 1, 2, \dots, n-1 \quad (6)$$

Equation (5) is an extended version of the variance estimator given in (García-Fiñana & Cruz-Orive, 2004).

Section (i)	P_i	P_i^2	$P_i \cdot P_{i+1}$	$P_i \cdot P_{i+2}$	$P_i \cdot P_{i+4}$
1	42	1764	3024	5124	5418
2	72	5184	8784	9504	8352
3	122	14884	16104	15738	14030
4	132	17424	17028	15312	8976
5	129	16641	14964	14835	0
6	116	13456	13340	7888	0
7	115	13225	7820	0	0
8	68	4624	0	0	0
		87202	81064	68401	36776
Total	796	C_0	C_1	C_2	C_4

Table 2. Calculation of the constants C_0, C_1, C_2, C_4

The smoothness constant can be estimated from Eq. (7) as follows:

$$q = \max \left\{ 0, \frac{1}{2 \log 2} \log \left[\frac{(3C_0 - 4C_2 + C_4)}{(3C_0 - 4C_1 + C_2)} \right] - \frac{1}{2} \right\} \tag{7}$$

$$q = \left\{ 0, \frac{1}{2 \log 2} \log \left[\frac{3 \times 87202 - 4 \times 68401 + 36776}{3 \times 87202 - 4 \times 81064 + 68401} \right] - \frac{1}{2} \right\} = 0.53$$

We apply Eq. (7) with $\alpha = 0.53$.

The coefficient $\alpha(q)$ has the following expression (Eq.8):

$$\alpha(q) = \frac{\Gamma(2q+2)\zeta(2q+2)\cos(\pi q)}{(2\pi)^{2q+2}(1-2^{2q-1})} \quad q \in [0,1] \tag{8}$$

where Γ and ζ denote the gamma function and the Riemann Zeta function, respectively.

$$a(0.53) = \frac{\Gamma(2.06)\zeta(2.06)\cos(1.66)}{(2\pi)^{2.06}(1-2^{0.06})} = 0.018$$

Therefore, the estimate of $\text{Var}(\hat{Q}_T)$ obtained via Eq. (5) is:

$$\begin{aligned} \text{var}(Q_T) &= a(q)(3C_0 - 4C_1 + C_2)T^2 \\ \text{var}(Q_T) &= 0.018 \times (3 \times 87202 - 4 \times 81064 + 68401) \times (1.6)^2 \\ \text{var}(Q_T) &= 9.2 \end{aligned} \tag{9}$$

We predict the value of CE;

$$CE(Q_T) = \sqrt{9.2 / 856.9} = 0.0103 = 1.03\%$$

In our studies, we calculate the CE values as predictive using the R program. First, by using the statistical package R, codes are developed to calculate the contribution to the predictive

CE (García-Fiñana & Cruze-Orive, 2004). A value of CE lower than 5% is in the acceptable range (Gundersen & Jensen, 1987, and 1999; Sahin et al., 2003). In addition, it is very important to note that an appropriate grid size and the number of slices required for volume estimation of an object is crucial at the beginning.

5. Conclusion

In conclusion, MRI may help to specify the cause of the disease such as the brain atrophy, if a kind of neurodegenerative disease is present. Unfortunately, however, conventional MRI study not give substructural detailed information about cellular and molecular organisation of the brain tissue. On the other hand, it is also possible to define the etiologies of the pathologies using new functional MRI methods, such as diffusion weighted imaging and MRS. Future advances in functional and anatomic neuroimaging techniques provide further insights into certain neurodegenerative diseases of the brain. A combination of different neuroimaging techniques and atrophy correction through MRI, PET and SPECT superimposition may demonstrate functional and morphological features of the brain tissue. In similar to MRI, PET and SPECT are useful in the diagnosis of some neurodegenerative diseases.

By using MRI, the estimation of the brain volume is a well-known entity for the determination of the brain atrophy. Several different methods such as segmentation techniques are available for the estimation of the brain volume, but there are only a few stereological studies using point-counting and planimetric methods. Recently, the Cavalieri principle in combination with point-counting has become popular in the understanding of the pathologies of brain morphology. There is no doubt that determination of the brain atrophy using MRI will be useful in understanding of neurodegenerative diseases, monitoring of disease progression, and treatment of such patients. In conclusion, the Cavalieri principle in combination with point-counting is an ideal method for the estimation of total volume of the brain or any of its compartment for the diagnosis of atrophic neurodegenerative diseases.

Nevertheless, further combinations of new imaging techniques with different methods for volume estimation using a combination of different neuroimaging techniques are needed for early diagnosis and monitorization of course of the disease. It is important to know that these techniques for volume estimation must be reproducible and reliable. The greater accuracy of imaging methods in detection of early neurodegenerative diseases will result in early optimal treatment to delay further cognitive decline.

6. References

- Acer, N.; Sahin, B.; Baş, O.; Ertekin, T. & Usanmaz, M. (2007). Comparison of three methods for the estimation of total intracranial volume: stereologic, planimetric, and anthropometric approaches. *Ann Plast Surg* Vol. 58, No. 1, (Jan 2007), pp. 48-53. ISSN 0148-7043
- Acer, N.; Sahin, B.; Usanmaz, M., Tatoğlu, H. & Irmak, Z. (2008). Comparison of point counting and planimetry methods for the assessment of cerebellar volume in human using magnetic resonance imaging: a stereological study. *Surg Radiol Anat* Vol. 30, No. 4, (Jun 2008), pp. 335-9. ISSN 0930-1038

- Acer, N.; Uğurlu, N.; Uysal, DD.; Unur, E.; Turgut, M. & Camurdanoğlu, M. (2010). Comparison of two volumetric techniques for estimating volume of intracerebral ventricles using magnetic resonance imaging: a stereological study. *Anat Sci Int* Vol. 85, No. 3, (Sep 2010), pp. 131-9. ISSN 1447-6959
- Ahmed, MN.; Yamany, SM.; Mohamed, N.; Farag, AA. & Moriarty, T. (2002). A modified fuzzy c-means algorithm for bias field estimation and segmentation of MRI data. *EEE Trans Med Imag* Vol. 21, No. 3, (Mar 2002), pp. 193-199. ISSN 0278-0062
- Amato, U.; Larobina, M.; Antoniadis, A. & Alfano, B. (2003). Segmentation of magnetic resonance brain images through discriminant analysis. *J Neurosci Methods* Vol. 131, No. 1-2, (Dec 2003), pp 65-74. ISSN 0165-0270
- Appel, J.; Potter, E.; Shen, Q.; Pantol G.; Greig, MT.; Loewenstein, D. & Duara, R. (2009). A comparative analysis of structural brain MRI in the diagnosis of Alzheimer's disease. *Behav Neurol* Vol. 21, No. 1, (Oct 2009), pp. 13-19, ISSN 0953-4180
- Ashburner, J. & Friston, KJ. (2005). Unified segmentation. *NeuroImage* Vol. 26, No. 3, (Jul 2005), pp. 839-851. ISSN 1053-8119
- Belliveau JW, Kennedy DN, McKinstry RC, Buchinder, BR; Weiskoff, RM; Cohen, MS; Vevea, JM, Brady, TJ. & Rosen BR. (1992). Functional mapping of the human visual cortex by magnetic resonance imaging. *Science* Vol. 254, No. 5032, (Nov 1991), pp. 716-719. ISSN 0036-8075
- Basser, PJ.; Mattiello, J. & LeBihan, D. (1994). MR diffusion tensor spectroscopy and imaging. *Biophysics Journal* Vol. 66, No. 1 (Jan 1994), pp. 259-267, ISSN 0006-3495/94/01/259/09
- Bermel, RA.; Sharma, J.; Tjoa, CW.; Puli, SR. & Bakshi, R. (2003). A semiautomated measure of whole-brain atrophy in multiple sclerosis. *J Neurol Sci* Vol. 208, No. 1-2, (Apr 2003), pp. 57-65, ISSN 0022-510X
- Bothwell, JH. & Griffin JL. (2011). An introduction to biological nuclear magnetic resonance spectroscopy. *Biol Rev Camb Philos Soc* Vol. 86, No. 2, (May 2011), pp. 493-510, ISSN 0006-3231
- Brouwer, RM.; Hulshoff, PHE. & Schnack, HG. (2010). Segmentation of MRI brain scans using non-uniform partial volume densities. *NeuroImage* Vol. 49, No. 1, (Jan 2010), pp. 467-477, ISSN 1053-8119
- Bradley, WG. Jr. & Bydder, GM. (1997). *Advanced MR Imaging techniques*. Martin Dunitz Ltd, Informa Healthcare; 1 ed., London. ISBN 978-1853170249
- Boone, KB.; Miller, BL.; Lesser, IM.; Mehninger, CM.; Hill-Gutierrez, E.; Goldberg, MA. & Berman, NG. (1992). Neuropsychological correlates of white-matter lesions in healthy elderly subjects. A threshold effect. *Arch Neurol* Vol. 49, No. 5, (May 1992), pp. 549-554, ISSN 0003-9942
- Bonilha, L.; Halford, JJ.; Rorden, C.; Roberts, DR.; Rumboldt, Z. & Eckert, MA. (2009). Automated MRI analysis for identification of hippocampal atrophy in temporal lobe epilepsy. *Epilepsia* Vol. 50, No. 2 (Feb 2009) pp. 228-233. ISSN 0013-9580
- Buchsbaum, MS.; Tang, CY.; Peled, S.; Gudbjartsson, H.; Lu, D.; Hazlett, EA.; Downhill, J.; Haznedar, M.; Fallon, JH. & Atlas SW. (1998). MRI white matter diffusion anisotropy and PET metabolic rate in schizophrenia. *Neuroreport* Vol. 9, No. 3 (Feb 1998), pp. 425-430, ISSN 0959-4965

- Creasey, H.; Schwartz, M.; Frederickson, H.; Haxby, JV. & Rapoport, SI. (1986). Quantitative computed tomography in dementia of the Alzheimer type. *Neurology* Vol. 36, No. 12 (Dec 1986), pp. 1563-1568. ISSN 0811-8663
- Chan-Palay, V. & Asan, E. (1989). Alterations in catecholamine neurons of the locus coeruleus in senile dementia of the Alzheimer type and in Parkinson's disease with and without dementia and depression. *J Comp Neurol* Vol. 287, No. 3, (Sep1989), pp. 373-392, ISSN 0021-9967
- Calmon, G. & Roberts, N. (2000). Automatic measurement of changes in brain volume on consecutive 3DMR images by segmentation propagation. *Magn Reson Imaging* Vol. 18, No.4 (May 2000), pp. 439-453, ISSN 0730-725X
- Cowell, PE.; Sluming, VA.; Wilkinson, ID.; Cezayirli, E.; Romanowski, CA.; Webb, JA.; Keller, SS.; Mayes, A. & Roberts, N. (2007). Effects of sex and age on regional prefrontal brain volume in two human cohorts. *Eur J Neurosci* Vol. 25, No. 1 (Jan 2007), pp. 307-318, ISSN 0953-816X
- Dale, AM.; Fischl, B. & Sereno, MI. (1999). Cortical surface-based analysis I. Segmentation and surface reconstruction. *Neuroimage* Vol. 9, No. 2 (Feb 1999), pp. 179-194, ISSN 1053-8119
- Davatzikos, C.; Fan, Y.; Wu, X.; Shen, D. & Resnick, SM. (2008). Detection of prodromal Alzheimer's disease via pattern classification of magnetic resonance imaging. *Neurobiol Aging* Vol. 29, No. 4 (Apr 2008), pp. 514-523, ISSN 0197-4580
- Ewers M, Frisoni GB, Teipel SJ, Grinberg LT, Amaro E Jr, Heinsen H, Thompson PM. & Hampel H. (2011). Staging Alzheimer's disease progression with multimodality neuroimaging. *Prog Neurobiol* (in press). ISSN 0301-0082
- Fischl, B.; Sereno, MI. & Dale, AM. (1999). Cortical surface-based analysis. II: Inflation, flattening, and a surface-based coordinate system. *Neuroimage* Vol. 9, No. 2 (Feb 1999), pp. 195-207, ISSN 1053-8119
- Fischl, B., Salat, DH.; Busa, E.; Albert, M.; Dieterich, M.; Haselgrove, C.; van der Kouwe, A.; Killiany, R.; Kennedy, D.; Klaveness, S.; Montillo, A.; Makris, N.; Rosen, B. & Dale, AM. (2002). Whole brain segmentation: automated labeling of neuroanatomical structures in the human brain. *Neuron* Vol. 33, No. 3 (Jan 2002), pp. 341-355, ISSN 0896-6273
- Flippi, M.; Masrtonardo, G.; Rocca, MA.; Pereira, C. & Comi, G. (1998). Quantitative volumetric analysis of brain magnetic resonance imaging from patients with multiple sclerosis. *J Neurol Sci* Vol. 158, No. 2 (Jun 1998), pp. 148-153. ISSN 0022-510X
- Frey, H.; Lahtinen, A.; Heinonen, T. & Dastidar, P. (1999). Clinical Application of MRI Image Processing in Neurology *IJBEM* Vol. 1, No. 1 (May 1999), pp. 47-53, ISSN 1456-7865
- Furlong, C. (2008) Investigation of the precision and accuracy of surface area and volume estimators of the human brain using stereology and magnetic resonance. *Liverpool University. Doctorate Thesis*, (March 2008), England
- García-Fiñana, M.; Cruz-Orive, LM.; Mackay, CE.; Pakkenberg, B. & Roberts, N. (2003). Comparison of MR imaging against physical sectioning to estimate the volume of human cerebral compartments. *Neuroimage* Vol. 18, No. 2 (Feb 2003), pp. 505-516, ISSN 1053-8119
- García-Fiñana, M. (2006). Confidence intervals in Cavalieri sampling. *J Microsc* Vol. 222, No. 3, (Jun 2006), pp. 146-157, ISSN 0022-2720

- García-Fiñana, M.; Keller, SS. & Roberts, N. (2009). Confidence intervals for the volume of brain structures in Cavalieri sampling with local errors. *J Neurosci Methods* Vol. 179, No. 1 (Apr 2009), pp. 71-77, ISSN 0165-0270
- García-Fiñana M. & Cruze-Orive LM. (2004). Improved variance prediction for systematic on R. *Statistics* Vol. 38, No. 3, pp. 243-272, ISSN 0233-1888
- García-Fiñana, M. & Cruz-Orive, LM. (2000). New approximations for the variance in cavalieri sampling. *J Microsc* Vol. 199, No. 2 (Sep 2000), pp. 224-238, ISSN 0022-2720
- Geuze, E.; Vermetten, E. & Bremner, JD. (2005). MR-based in vivo hippocampal volumetrics: 1. Review of methodologies currently employed. *Mol Psychiatry* Vol. 10, No. 2 (Feb 2005), pp. 147-159, ISSN 1359-4184
- Gundersen, HJ. & Jensen, EB. (1987). The efficiency of systematic sampling in stereology and its prediction. *J Microsc* Vol. 147, No. 3 (Sep 1987), pp. 229-263, ISSN 0022-2720
- Gomez-Isla, T.; Hollister, R.; West, H.; Mui, S.; Growdon, JH.; Petersen, RC.; Parisi, JE. & Hyman, BT. (1997). Neuronal loss correlates with but exceeds neurofibrillary tangles in Alzheimer's disease. *Ann Neurol* Vol. 41, No. 1 (Jan 1997), pp. 17-24, ISSN 0364-5134
- Gomez-Isla, T.; Price, JL.; McKeel, DW Jr.; Morris, JC.; Growdon, JH. & Hyman, BT. (1996). Profound loss of layer II entorhinal cortex neurons occurs in very mild Alzheimer's disease. *J Neurosci* Vol. 16, No. 14 (Jul 1996), pp. 4491-4500, ISSN 0270-6474
- Grassiot, B.; Desgranges, B.; Eustache, F. & Defer, G. (2009). Quantification and clinical relevance of brain atrophy in multiple sclerosis: a review. *J Neurol* Vol. 256, No. 9 (Sep 2009), pp. 1397-1412, ISSN 0340-5354
- Gundersen, HJ.; Jensen, EB.; Kiêu, K. & Nielsen, J. (1999). The efficiency of systematic sampling in stereology reconsidered. *J Microsc* Vol. 193, No. 4 (Mar 1999), pp. 199-211, ISSN 0022-2720
- Hanyu, H.; Shindo, H.; Kakizaki D.; Abe, K.; Iwamoto, T. & Takasaki M. (1997). Increased water diffusion in cerebral white matter in Alzheimer's disease. *Gerontology* Vol. 43, No. 6 (Oct 24, 1996), pp. 343-351, ISSN 0304-324X
- Henry, TR.; Chupin, M.; Lehericy, S.; Strupp, JP.; Sikora, MA.; Sha, ZY.; Ugurbil, K. & Van de Moortele, PF. (2011). Hippocampal sclerosis in temporal lobe epilepsy: findings at 7 T. *Radiology* (in press). [Epub ahead of print]. ISSN 0033-8419
- Horsfield, MA.; Rovaris, M.; Rocca, MA.; Rossi, P.; Benedict, RH.; Filippi, M. & Bakshi, R. (2003). Whole-brain atrophy in multiple sclerosis measured by two segmentation processes from various MRI sequences. *Neurol Sci* Vol. 216, No. 1 (Dec 2003), pp. 169-177, ISSN 0020-510X
- Houtchens, MK.; Benedict, RH.; Killiany, R.; Sharma, J.; Jaisani, Z., Singh, B.; Weinstock-Guttman, B.; Guttmann, CR. & Bakshi, R. (2007). Thalamic atrophy and cognition in multiple sclerosis. *Neurology* Vol. 69, No. 17 (Sep 2007), pp. 1213-1223, ISSN 0028-3878
- Herndon, RC., Lancaster, JL., Giedd, JN. & Fox, PT. (1998). Quantification of white matter and gray matter volumes from three-dimensional magnetic resonance golumes studies using fuzzy classifiers. *J Magn Reson Imaging* Vol. 8, No. 5 (Sep 1998), pp. 1097-1005, ISSN 1053-1807
- Jones, EK.; Simmons, A.; Williams, SCR. & Horsfield, MA. (1999). Non-invasive assessment of axonal fiber connectivity in the human brain via diffusion tensor MRI. *Magn Reson Med* Vol. 42, No. 1 (July 1999), pp. 37-41, ISSN 1522-2594

- Keller, SS. & Roberts, N. (2009). Measurement of brain volume using MRI: software, techniques, choices and prerequisites. *Journal of Anthropological Sciences* Vol. 87, pp. 127-151, ISSN 1827-4765
- Keller, SS.; Mackay, CE.; Barrick, TR.; Wieshmann, UC.; Howard, MA. & Roberts N. (2002). Voxel-based morphometric comparison of hippocampal and extrahippocampal abnormalities in patients with left and right hippocampal atrophy. *Neuroimage* Vol. 16, No. 1 (May 2002), pp. 23-31, ISSN 1053-8119
- Keller SS.; Highley JR.; Garcia-Finana M.; Sluming V.; Rezaie R. & Roberts N. (2007). Sulcal variability, stereological measurement and asymmetry of Broca's area on MR images. *J Anat* Vol. 211, No. 4 (Oct 2007), pp. 534-555, ISSN 0021-8782
- Keller, SS & Roberts, N. (2008). Voxel-based morphometry of temporal lobe epilepsy: An introduction and review of the literature. *Epilepsia* (May 2008), Vol. 49, No. 5, pp. 741-757, ISSN 0013-9580
- Kern, A. & Behl, C. (2009). The unsolved relationship of brain aging and late-onset Alzheimer disease *Biochimica et Biophysica Acta (BBA)* Vol. 1790, No. 10, (Oct 2009), pp. 1124-1132, ISSN 0304-4165
- Kesslak, JP.; Nalcioglu, O. & Cotman, CW. (1991). Quantification of magnetic resonance scans for hippocampal and parahippocampal atrophy in Alzheimer's disease. *Neurology* Vol. 41, No. 1 (Jan 1991), pp. 51-54, ISSN 0811-8663
- Kucharczyk, W. & Henkelman, M. (1994). Visibility of Calcium on MR and CT: can MR show calcium that CT can not?. *AJNR Am J Neuroradiol*. Vol. 15, No. 6 (Jun 1994), pp. 1145-1148, ISSN 0195-6108
- Likeman, M.; Anderson, VM.; Stevens, JM.; Waldman, AD.; Godbolt, AK.; Frost, C.; Rossor, MN. & Fox, NC. (2005). Visual assessment of atrophy on magnetic resonance imaging in the diagnosis of pathologically confirmed young-onset demantias. *Arch Neurol* Vol. 62, No. 9 (Sept 2005), pp. 1410-1415, ISSN 0003-9942
- Lim, OK.; Rosenbloom, M. & Pfefferbaum, A. (2000). In Vivo Structural Brain Assessment: In: *Psychopharmacology-4th Generation of Progress*, Bloom FE, Kupfer DJ. (Ed.), Part II Clinic section, ISBN 978-0781701662.
<http://www.acnp.org/g4/GN401000089/Default.htm>
- Liu, YS.; Yi, J.; Zhang, H.; Zheng, G. & Paul, JC. (2010). Surface area estimation of digitized 3D objects using quasi-Monte Carlo methods. *Pattern Recogn*. Vol. 43, No. 11 (November 2010), pp. 3900-3909, ISSN 0031-3203
- Loewe, C.; Oschatz, E. & Prayer, D. (2002). Imaging of Neurodegenerative Disorders of the Brain in Adults. *Imaging Decisions* Vol. 6, Supplement 1 (Dec 2002), pp. 4-18, ISSN 1617-0830
- Lopez, OL.; Becker, JT.; Rezek, D.; Wess, J.; Boller F.; Reynolds CF, 3rd. & Panisset, M. (1992). Neuropsychiatric correlates of cerebral white-matter radiolucencies in probable Alzheimer's disease. *Arch Neurol* Vol. 49, No. 8 (Aug 1992), pp. 828-834, ISSN 0003-9942
- Mackay, CE.; Roberts, N.; Mayes, AR.; Downes, JJ.; Foster, JK. & Mann, D. (1998). An exploratory study of the relationship between face recognition memory and the volume of medial temporal lobe structures in healthy young males. *Behav Neurol* Vol. 11, No. 1 (Jan 1998), pp. 3-20, ISSN 0953-4180
- Masliah, E.; Terry, R.; Alford, M.; DeTeresa, R. & Hansen, LA. (1991). Cortical and subcortical patterns of synaptophysin-like immunoreactivity in Alzheimer's disease. *Am J Pathol* Vol. 138, No. 1 (Jan 1991), pp. 235-246, ISSN 0002-9440

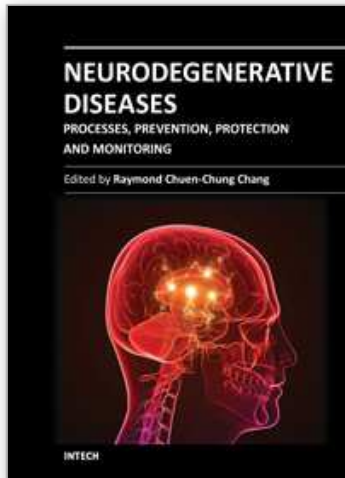
- Mazziotta, JC.; Frackowiak, RSJ. & Phelps, ME. (1992). The use of positron emission tomography in the clinical assessment of dementia. *Semin Nucl Med* Vol. 22, No. 4 (Oct 1992), pp. 233-246, ISSN 0001-2998
- McKhann, GM.; Albert, MS.; Grossman, M.; Miller, B.; Dickson, D. & Trojanowski, JQ. (2001). Clinical and pathological diagnosis of frontotemporal dementia: Report of the Work Group on Frontotemporal Dementia and Pick's Disease. *Arch Neurol* Vol. 58, No. 11 (Nov 2001), pp. 1803-1809, ISSN 0003-9942
- Mohamed, FB.; Vinitiski, S.; Faro, SH.; Gonzalez, CF.; Mack, J. & Iwanaga, T. (1999). Optimization of tissue segmentation of brain MR images based on multispectral 3D feature maps. *Magn. Reson. Imaging* Vol.17, No. 3 (Apr 1999), pp. 403-409, ISSN 0730-725X
- Mohs, RC. & Haroutunian, V. (2002) Chapter 82: Alzheimer Disease: From Earliest Symptoms to End Stage, *Neuropsychopharmacology*: pp. 1189-1197. Edited by Kenneth L. Davis, Dennis Charney, Joseph T. Coyle, and Charles Nemeroff. American College of Neuropsychopharmacology The Fifth Generation of Progress
- Molyneux, PD.; Kappos, L.; Polman, C.; Pozzilli, C.; Barkhof, F.; Filippi, M.; Yousry, T.; Hahn, D.; Wagner, K.; Ghazi, M.; Beckmann, K.; Dahlke, F.; Losseff, N.; Barker, GJ.; Thompson, AJ. & Miller, DH. (2000). The effect of interferon beta-1b treatment on MRI measures of cerebral atrophy in secondary progressive multiple sclerosis. European Study Group on Interferon Beta-1b in Secondary Progressive Multiple Sclerosis. *Brain* Vol. 123, No. 11 (Nov 2000), pp. 2256-2263, ISSN 0006-8950
- Nagy, Z.; Esiri, MM.; Jobst, KA.; Morris, JH.; King, EM.; McDonald, B.; Litchfield, S.; Smith, A.; Barnettson, L. & Smith, AD. (1995). Relative roles of plaques and tangles in the dementia of Alzheimer's disease: correlations using three sets of neuropathological criteria. *Dementia* Vol. 6, No. 1 (Jan 1995), pp. 21-31, ISSN 1013-7424
- Nakamura, K. & Fisher, E. (2009). Segmentation of brain magnetic resonance iamges for measuremnt of gray matter atrophy in multiple sclerosis patients. *Neuroimage* Vol. 44, No. 3 (Feb 2009), pp. 796-776, ISSN 1053-8119
- Neary, D.; Snowden, JS.; Gustafson, L.; Passant, U.; Stuss, D.; Black, S.; Freedman, M.; Kertesz, A.; Robert, PH.; Albert, M.; Boone, K.; Miller, BL.; Cummings, J. & Benson, DF. (1998). Frontotemporal lobar degeneration: A consensus on clinical diagnostic criteria. *Neurology* Vol. 51, No. 6 (Dec 1998), pp. 1546-1554, ISSN 0811-8663
- O'Brien, JT. (2007). Role of imaging techniques in the diagnosis of dementia. *Br J Radiol* Vol. 80, No. 2 (Dec 2007), pp. 71-77, ISSN 0007-1285
- O'Sullivan, M. (2009). Patterns of brain atrophy on magnetic resonance imaging and the boundary between ageing and Alzheimer's disease. *Rev Clin Gerontol* Vol. 19, No. 4 (Nov 2009), pp. 295-307, ISSN 0959-2598
- Pearlson, GD.; Harris, GJ.; Powers, RE.; Barta, PE.; Camargo, EE.; Chase, GA.; Noga, JT. & Tune, LE. (1992). Quantitative changes in mesial temporal volume, regional cerebral blood flow, and cognition in Alzheimer's disease. *Arch Gen Psychiatry* Vol. 49, No. 5 (May 1992), pp. 402-408. ISSN 0003-990X
- Pelletier, D.; Garrison, K. & Henry, R. (2004). Measurement of whole brain atrophy in multiple sclerosis. *J Neuroimaging* Vol. 14, No. 3 (Jul 2004), pp.11S-19S, ISSN 1051-2284
- Pham, DL. & Prince, JL. (1999). Adaptive fuzzy segmentation of magnetic resonance images. *IEEE Trans Med Imag* Vol. 18, No. 9 (Sep 1999), pp. 737-752, ISSN 0278-0062

- Ratnavalli, E.; Brayne, C.; Dawson, K. & Hodges, JR. (2002). The prevalence of frontotemporal dementia. *Neurology* Vol. 58, No. 11 (Jun 2002), pp. 1615-1621. ISSN 0811-8663
- Rusinek, H.; de Leon, MJ.; George, AE.; Stylopoulos, LA.; Chandra, R.; Smith, G.; Rand, T.; Mourino, M. & Kowalski, H. (1991). Alzheimer disease: measuring loss of cerebral gray matter with MR imaging. *Radiology* Vol. 178, No. 1 (Jan 1991), pp. 109-114. ISSN 0033-8419
- Rosen, HJ.; Gorno-Tempini, ML.; Goldman, WP.; Perry, RJ.; Schuff, N.; Weiner, M.; Feiwell, R.; Kramer, JH. & Miller, BL. (2002). Patterns of brain atrophy in frontotemporal dementia and semantic dementia. *Neurology* Vol. 58, No. 2 (Jan 2002), pp. 198-208. ISSN 0811-8663
- Rosen, HJ.; Allison, SC.; Schauer, GF.; Gorno-Tempini, ML.; Weiner, MW. & Miller, BL. (2005). Neuroanatomical correlates of behavioural disorders in dementia. *Brain* Vol. 128, No. 11 (Nov 2005), pp. 2612-2625. ISSN 0006-8950
- Rosen, HJ.; Wilson, MR.; Schauer, GF.; Allison S.; Gorno-Tempini ML.; Pace-Savitsky C.; Kramer JH.; Levenson RW.; Weiner M. & Miller BL. (2006). Neuroanatomical correlates of impaired recognition of emotion in dementia. *Neuropsychologia* Vol. 44, No. 3 (Sep 2005), pp. 365-373, ISSN 0028-3932
- Ron, MA.; Acker, W.; Shaw, GK. & Lishman, WA. (1982). Computerized tomography of the brain in chronic alcoholism: a survey and follow-up study. *Brain* Vol. 105, No. 3 (Sep 1982), pp. 497-514. ISSN 0006-8950
- Roberts, N.; Puddephat, MJ. & McNulty, V. (2000). The benefit of stereology for quantitative radiology. *Br J Radiol* Vol. 73, No. 871 (Jul 2000), pp. 679-697, ISSN 0007-1285.
- Sahin, B. & Ergur, H. (2006). Assessment of the optimum section thickness for the estimation of liver volume using magnetic resonance images: a stereological gold standard study. *Eur J Radiol* Vol. 57, No. 1 (Jan 2006), pp. 96-101. ISSN 0720-04X
- Sahin, B.; Emirzeoglu, M.; Uzun, A.; Incesu, L.; Bek, Y.; Bilgic, S. & Kaplan, S. (2003). Unbiased estimation of the liver volume by the Cavalieri principle using magnetic resonance images. *Eur J Radiol* Vol. 47, No. 2 (Aug 2003), pp. 164- 170, ISSN 0720-04X
- Sanfilipo, MP.; Benedict, RH.; Sharma, J.; Weinstock-Guttman, B. & Bakshi, R. (2005). The relationship between whole brain volume and disability in multiple sclerosis: a comparison of normalized gray vs white matter with misclassification correction. *Neuroimage* Vol. 26, No. 4 (July 2005), pp. 1068-1077. ISSN 1053-8119
- Sanfilipo, MP.; Benedict, RH.; Weinstock-Guttman, B. & Bakshi, R. (2006). Gray and white matter brain atrophy and neuropsychological impairment in multiple sclerosis. *Neurology* Vol. 66, No. 5 (Mar 2006), pp. 685-692, ISSN 0811-8663
- Schuckit, MA. (1992). An introduction and overview of clinical applications of NeuroSPECT in psychiatry. *J Clin Psychiatry* Vol. 53, Suppl (November 1992), pp. 3-6, ISSN 0160-6689
- Schuff, N.; Amend, D.; Ezekiel, F.; Steinman, SK.; Tanabe, J.; Norman, D.; Jagust, W.; Kramer, JH.; Mastrianni, JA.; Fein, G. & Weiner, MW. (1997). Changes of hippocampal N-acetyl aspartate and volume in Alzheimer's disease: a proton MR spectroscopic imaging and MRI study. *Neurology* Vol. 49, No. 6, pp. 1513-1521. ISSN 0811-8663

- Seppi, K. & Schocke, MF. (2005). An update on conventional and advanced magnetic resonance imaging techniques in the differential diagnosis of neurodegenerative parkinsonism. *Curr Opin Neurol* Vol. 18, No. 4 (Aug 2005), pp. 370–375. ISSN 1350-7540
- Sharma, J.; Sanfilippo, MP.; Benedict, RH.; Weinstock-Guttman, B.; Munschauer, FEIII. & Bakshi, R. (2004). Whole-brain atrophy in multiple sclerosis measured by automated versus semiautomated MR imaging segmentation. *AJNR Am J Neuroradiol* Vol. 25, No. 6 (Jun 2004), pp. 985–996, ISSN 0195-6108
- Small, GW. (2002). Structural And Functional Brain Imaging of Alzheimer Disease. *Neuropsychopharmacology: The Fifth Generation of Progress*, Davis, KL.; Charney, D.; Joyle, J. (Ed). pp. 1232-1242. ISBN 978-0781728379.
- Smith, SM.; Zhang, Y.; Jenkinson, M.; Chen, J.; Matthews, PM.; Federico, A. & De Stefano, N. (2002). Accurate, robust, and automated longitudinal and cross-sectional brain change analysis, *Neuroimage* Vol. 17, No. 1 (Sep 2002), pp. 479–489, ISSN 1053-8119
- Stokking, R.; Vincken, KL. & Viergever, MA. (2000). Automatic morphology-based brain segmentation (MBRASE) from MRI-T1 data. *Neuroimage* Vol. 12, No. 6 (Dec 2000), pp. 726–738, ISSN 1053-8119
- Suckling, J.; Sigmundsson, T.; Greenwood, K. & Bullmore, ET. (1999). A modified fuzzy clustering algorithm for operator independent brain tissue classification of dual echo MR images. *Magn Reson Imaging* Vol. 17, No. 7 (Sep 1999), pp. 1065–1076, ISSN 0730-725X
- Suri, JS.; Setarehdan, SK. & Singh, S. (2002). Advanced Algorithmic Approaches to Medical Image Segmentation: *State-of-the-Art Applications in Cardiology, Neurology, Mammography and Pathology*. Springer-Verlag, London/Berlin/Heidelberg, ISBN 978-1-85233-389-8
- Terry, RD.; Peck, A.; DeTeresa, R.; Schechter, R. & Horoupian, DS. (1981). Some morphometric aspects of the brain in senile dementia of the Alzheimer type. *Ann Neurol* Vol. 10, No. 2 (Aug 1981), pp. 184–192, ISSN 0364-5134
- Teipel, SJ.; Bayer, W.; Alexander, GE.; Bokde, AL.; Zebuhr, Y.; Teichberg, D.; Müller-Spahn, F.; Schapiro, MB.; Möller, HJ.; Rapoport, SI. & Hampel, H. (2003). Regional pattern of hippocampus and corpus callosum atrophy in Alzheimer's disease in relation to dementia severity: evidence for early neocortical degeneration. *Neurobiol Aging* Vol. 24, No. 1 (Jan 2003), pp. 85–94, ISSN 0197-4580
- Tosun, D.; Rettmann, ME.; Han, X.; Tao, X., Xu, C.; Resnick, SM., Dzung, LP. & Prince, JL. (2004). Cortical surface segmentation and mapping, *NeuroImage* Vol. 23, Suppl. 1, pp. 108-118, ISSN 1053-8119
- Ueda, K.; Fujiwara, H.; Miyata, J.; Hirao, K.; Saze, T.; Kawata, R.; Fujimoto, S., Tanaka, Y., Sawamoto, N.; Fukuyama, H. & Murai T. (2009). Investigating association of brain volumes with intracranial capacity in schizophrenia. *Neuroimage* Vol. 19, No. 3, (Sep 2009), pp. 2503-2508, ISSN 1053-8119
- Vitali, P.; Migliaccio, R.; Agosta, F.; Rosen, HJ. & Geschwind, MD. (2008). Neuroimaging in dementia. *Semin Neurol* Vol. 28, No. 4, pp. 467-483. ISSN 0271-8235
- Wagner, AD.; Schacter, DL.; Rotte, M.; Koutstaal, W.; Maril, A.; Dale, AM.; Rosen, BR. & Buckner, RL. (1998). Building memories: remembering and forgetting of verbal experiences as predicted by brain activity. *Science* Vol. 281, No. 5380 (Aug 1998), pp.1188-1191, ISSN 0036-8075

- Webb, J.; Guimond, A., Eldridge, P.; Chadwick, D.; Meunier, J. & Thirion, JP. (1999). Automatic detection of hippocampal atrophy on magnetic resonance images. *Magn Reson Imaging* Vol. 17, No. 8 (Oct 1999), pp. 1149–1161, ISSN 0730-725X
- Weiner, MW. (1987). NMR spectroscopy for clinical medicine, animal models, and clinical examples. *Ann NY Acad Sci* Vol. 508, (November 1987), pp. 287–289, ISSN 1749-6632
- Whitehouse, PJ.; Price, DL.; Struble, RG.; Clark, AW.; Coyle, JT. & Delon, MR. (1982). Alzheimer's disease and senile dementia: loss of neurons in the basal forebrain. *Science* Vol. 215, No. 4537 (Mar 1982), pp. 1237–1239, ISSN 0036-8075
- Yamauchi, H.; Fukuyama, H.; Nagahama, Y.; Katsumi, Y.; Hayashi, T.; Oyanagi, C.; Konishi, J. & Shio, H. (2000). Comparison of the pattern of atrophy of the corpus callosum in frontotemporal dementia, progressive supranuclear palsy, and Alzheimer's disease. *J Neurol Neurosurg Psychiatry* Vol. 69, No. 5, (Nov 2000), pp. 623–629, ISSN 0022-3050
- Zweig, RM.; Ross, CA.; Hedreen, JC.; Steele, C.; Cardillo, JE.; Whitehouse, PJ.; Folstein, MF. & Price, DL. (1988). The neuropathology of aminergic nuclei in Alzheimer's disease. *Ann Neurol* Vol. 24, No. 2, (Aug 1988), pp. 233–242, ISSN 0364-5134
- Zhou, Y. & Bai, J. (2007). Atlas-based fuzzy connectedness segmentation and intensity nonuniformity correction applied to brain MRI. *IEEE Trans. Biomed Eng* Vol. 54, No. 1, pp. 122–129, ISSN 0278-0062

IntechOpen



Neurodegenerative Diseases - Processes, Prevention, Protection and Monitoring

Edited by Dr Raymond Chuen-Chung Chang

ISBN 978-953-307-485-6

Hard cover, 558 pages

Publisher InTech

Published online 09, December, 2011

Published in print edition December, 2011

Neurodegenerative Diseases - Processes, Prevention, Protection and Monitoring focuses on biological mechanisms, prevention, neuroprotection and even monitoring of disease progression. This book emphasizes the general biological processes of neurodegeneration in different neurodegenerative diseases. Although the primary etiology for different neurodegenerative diseases is different, there is a high level of similarity in the disease processes. The first three sections introduce how toxic proteins, intracellular calcium and oxidative stress affect different biological signaling pathways or molecular machineries to inform neurons to undergo degeneration. A section discusses how neighboring glial cells modulate or promote neurodegeneration. In the next section an evaluation is given of how hormonal and metabolic control modulate disease progression, which is followed by a section exploring some preventive methods using natural products and new pharmacological targets. We also explore how medical devices facilitate patient monitoring. This book is suitable for different readers: college students can use it as a textbook; researchers in academic institutions and pharmaceutical companies can take it as updated research information; health care professionals can take it as a reference book, even patients' families, relatives and friends can take it as a good basis to understand neurodegenerative diseases.

How to reference

In order to correctly reference this scholarly work, feel free to copy and paste the following:

Niyazi Acer, Ahmet Tuncay Turgut, Yelda Ozsunar and Mehmet Turgut (2011). Quantification of Volumetric Changes of Brain in Neurodegenerative Diseases Using Magnetic Resonance Imaging and Stereology, Neurodegenerative Diseases - Processes, Prevention, Protection and Monitoring, Dr Raymond Chuen-Chung Chang (Ed.), ISBN: 978-953-307-485-6, InTech, Available from:

<http://www.intechopen.com/books/neurodegenerative-diseases-processes-prevention-protection-and-monitoring/quantification-of-volumetric-changes-of-brain-in-neurodegenerative-diseases-using-magnetic-resonance>

INTECH
open science | open minds

InTech Europe

University Campus STeP Ri
Slavka Krautzeka 83/A
51000 Rijeka, Croatia

InTech China

Unit 405, Office Block, Hotel Equatorial Shanghai
No.65, Yan An Road (West), Shanghai, 200040, China
中国上海市延安西路65号上海国际贵都大饭店办公楼405单元

www.intechopen.com

Phone: +385 (51) 770 447
Fax: +385 (51) 686 166
www.intechopen.com

Phone: +86-21-62489820
Fax: +86-21-62489821

IntechOpen

IntechOpen

© 2011 The Author(s). Licensee IntechOpen. This is an open access article distributed under the terms of the [Creative Commons Attribution 3.0 License](#), which permits unrestricted use, distribution, and reproduction in any medium, provided the original work is properly cited.

IntechOpen

IntechOpen